



# Influence of DNA End Structure on the Mechanism of Initiation of DNA Unwinding by the *Escherichia coli* RecBCD and RecBC Helicases

Colin G. Wu and Timothy M. Lohman\*

Department of Biochemistry  
and Molecular Biophysics,  
Washington University School  
of Medicine, 660 South Euclid  
Avenue, Box 8231, St. Louis,  
MO 63110, USA

Received 17 April 2008;

received in revised form

2 July 2008;

accepted 3 July 2008

Available online

16 July 2008

*Escherichia coli* RecBCD is a bipolar DNA helicase possessing two motor subunits (RecB, a 3'-to-5' translocase, and RecD, a 5'-to-3' translocase) that is involved in the major pathway of recombinational repair. Previous studies indicated that the minimal kinetic mechanism needed to describe the ATP-dependent unwinding of blunt-ended DNA by RecBCD *in vitro* is a sequential *n*-step mechanism with two to three additional kinetic steps prior to initiating DNA unwinding. Since RecBCD can "melt out" ~6 bp upon binding to the end of a blunt-ended DNA duplex in a Mg<sup>2+</sup>-dependent but ATP-independent reaction, we investigated the effects of noncomplementary single-stranded (ss) DNA tails [3'-(dT)<sub>6</sub> and 5'-(dT)<sub>6</sub> or 5'-(dT)<sub>10</sub>] on the mechanism of RecBCD and RecBC unwinding of duplex DNA using rapid kinetic methods. As with blunt-ended DNA, RecBCD unwinding of DNA possessing 3'-(dT)<sub>6</sub> and 5'-(dT)<sub>6</sub> noncomplementary ssDNA tails is well described by a sequential *n*-step mechanism with the same unwinding rate ( $mk_U = 774 \pm 16 \text{ bp s}^{-1}$ ) and kinetic step size ( $m = 3.3 \pm 1.3 \text{ bp}$ ), yet two to three additional kinetic steps are still required prior to initiation of DNA unwinding ( $k_C = 45 \pm 2 \text{ s}^{-1}$ ). However, when the noncomplementary 5' ssDNA tail is extended to 10 nt [5'-(dT)<sub>10</sub> and 3'-(dT)<sub>6</sub>], the DNA end structure for which RecBCD displays optimal binding affinity, the additional kinetic steps are no longer needed, although a slightly slower unwinding rate ( $mk_U = 538 \pm 24 \text{ bp s}^{-1}$ ) is observed with a similar kinetic step size ( $m = 3.9 \pm 0.5 \text{ bp}$ ). The RecBC DNA helicase (without the RecD subunit) does not initiate unwinding efficiently from a blunt DNA end. However, RecBC does initiate well from a DNA end possessing noncomplementary twin 5'-(dT)<sub>6</sub> and 3'-(dT)<sub>6</sub> tails, and unwinding can be described by a simple uniform *n*-step sequential scheme, without the need for the additional  $k_C$  initiation steps, with a similar kinetic step size ( $m = 4.4 \pm 1.7 \text{ bp}$ ) and unwinding rate ( $mk_{\text{obs}} = 396 \pm 15 \text{ bp s}^{-1}$ ). These results suggest that the additional kinetic steps with rate constant  $k_C$  required for RecBCD to initiate unwinding of blunt-ended and twin (dT)<sub>6</sub>-tailed DNA reflect processes needed to engage the RecD motor with the 5' ssDNA.

© 2008 Elsevier Ltd. All rights reserved.

Edited by D. E. Draper

Keywords: helicase; recombination; motor protein; fluorescence; kinetics

## Introduction

DNA helicases are a diverse class of nucleic acid motor proteins that function by coupling the binding

and hydrolysis of 5'-NTP to translocation along the DNA filament and unwinding of duplex DNA in order to form the single-stranded (ss) intermediates required for DNA replication, recombination, and repair.<sup>1–7</sup> Some helicases can also displace other proteins from the nucleic acid.<sup>8–12</sup> Because helicase function is involved in all aspects of DNA metabolism, defects in human helicases can give rise to genetic disorders, such as Bloom syndrome, Werner syndrome, Rothmund–Thomson syndrome, and xeroderma pigmentosum, among others.<sup>13–16</sup>

\*Corresponding author. E-mail address:

lohman@biochem.wustl.edu.

Abbreviations used: ss, single stranded; ds, double stranded; FRET, fluorescence resonance energy transfer; NLLS, nonlinear least squares; BSA, bovine serum albumin.

In *Escherichia coli*, the RecBCD pathway is the major pathway for homologous recombination and repair of double-stranded (ds) DNA breaks. RecBCD is an essential DNA helicase for this pathway and is composed of the RecB (134 kDa), RecC (129 kDa), and RecD (67 kDa) polypeptides.<sup>17–19</sup> This heterotrimeric enzyme processes dsDNA breaks with its dsDNA and ssDNA exonuclease, ssDNA endonuclease, DNA-dependent ATPase, and helicase activities, which are regulated by the crossover hotspot instigator (*chi*) regulatory sequence (5'-GCTGGTGG-3').<sup>20–23</sup> RecBCD first binds to the damaged induced dsDNA break at a blunt or nearly blunt end and then unwinds the duplex in an ATP-dependent reaction. During DNA unwinding, its nuclease activity preferentially degrades the 3' terminating DNA strand while cleaving the 5' terminating strand infrequently.<sup>24,25</sup> These activities are modified when RecBCD recognizes a *chi* sequence, whereupon RecBCD first pauses and then continues to unwind DNA with a reduced rate.<sup>26–28</sup> Furthermore, the nuclease activity is altered such that it acts instead on the 5' terminating strand preferentially. This generates a 3' ssDNA overhang onto which RecBCD loads the RecA protein,<sup>29</sup> and the resulting RecA-coated DNA filament forms a joint molecule with a homologous piece of DNA and initiates recombinational repair of the nucleic acid.

RecB and RecD are both superfamily-1 helicases/translocases,<sup>30</sup> with opposite ssDNA translocation directionalities. Although the two motor subunits have opposite ssDNA translocation polarities (RecB is a 3'-to-5' translocase, while RecD is a 5'-to-3' translocase), they function in unison to unwind dsDNA in the same net direction within the RecBCD heterotrimer by interacting with opposite strands of the DNA end.<sup>31,32</sup> Interestingly, the RecBC enzyme, lacking the RecD subunit, is still a functional helicase. Both RecBCD and RecBC are processive helicases<sup>26,33,34</sup> that form stable heterotrimers and heterodimers, respectively, in solution.<sup>35–37</sup>

Equilibrium binding studies have indicated that RecBCD binds optimally to DNA ends possessing noncomplementary 5'-(dT)<sub>10</sub> and 3'-(dT)<sub>6</sub> ssDNA tails, while the RecBC binds optimally to DNA ends with 5'-(dT)<sub>6</sub> and 3'-(dT)<sub>6</sub> tails.<sup>37</sup> These results indicate that both the RecBCD and RecBC helicases are able to “melt out” 6 bp simply upon binding to a blunt-ended duplex in a Mg<sup>2+</sup>-dependent but ATP-independent reaction.<sup>38</sup> In a crystal structure of a RecBCD–DNA complex, the last 4 bp are observed to be melted even though the complex was crystallized in the presence of Ca<sup>2+</sup>.<sup>39</sup> Furthermore, the equilibrium binding studies suggest that additional 4 nt in the noncomplementary 5' ssDNA tail are needed to facilitate interactions with the RecD subunit.<sup>37</sup>

Lucius *et al.*<sup>40–42</sup> previously determined a minimal kinetic mechanism by which RecBCD unwinds blunt-ended DNA duplexes *in vitro* using rapid kinetic methods under single-turnover conditions. A simple uniform *n*-step sequential scheme was not able to describe the time courses for RecBCD unwinding of blunt-ended DNA. In fact, the minimal kinetic

mechanism required two to three additional kinetic steps, which made determination of the average DNA unwinding kinetic step size more difficult, although a well-constrained kinetic step size of  $3.9 \pm 0.5$  bp that was independent of ATP concentration and temperature was determined.<sup>40</sup> The number (two to three) of these additional steps was found to be independent of DNA duplex length, suggesting that these steps are not associated with the repeated cycles of DNA unwinding and likely precede or occur at the early stages of DNA unwinding.<sup>42</sup> Here, we examine the effects of noncomplementary 3' and 5' ssDNA tails on the mechanism by which RecBCD and RecBC initiate and processively unwind DNA in order to probe the role of RecD in the initiation of DNA unwinding.

## Results

The DNA substrates used in this study are shown schematically in Fig. 1, and the sequences of the individual DNA strands are given in Table 1. They consist of a DNA duplex containing two nicks with a hairpin structure on one end and noncomplementary ssDNA tails [(dT)<sub>*n*</sub>] on the other that forms the site at which RecBCD or RecBC will initiate unwinding. With the exception of the DNA substrate used in the experiments shown in Fig. 3, which possesses a blunt end, the 3' ssDNA tail length is 6 nt [(dT)<sub>6</sub>], while the 5' ssDNA length is either 6 nt [(dT)<sub>6</sub>] or 10 nt [(dT)<sub>10</sub>]. For the chemical quenched-flow unwinding experiments (see Fig. 2a), strand “A” is radiolabeled with <sup>32</sup>P on its 5' end (denoted as an asterisk in Fig. 1a). Displacement of the radioactively labeled DNA is used to monitor DNA unwinding in a discontinuous assay (see Materials and Methods). For the stopped-flow fluorescence experiments (see Fig. 2b), Cy3 and Cy5 fluorophores are positioned on either side of a nick (see Fig. 1b) and changes in Cy3 and Cy5 fluorescence resulting from changes in fluorescence resonance energy transfer (FRET) are used to monitor DNA unwinding. Both assays are “all-or-none” assays since DNA unwinding is not detected until duplex “A” (see Figs. 1 and 2) is fully unwound; however, information on intermediate species present during unwinding can be obtained by analyzing a series of unwinding experiments performed as a function of DNA duplex length.<sup>43,44</sup>

### RecBC initiates DNA unwinding poorly from a blunt DNA end

Single-turnover chemical quenched-flow kinetic studies were performed as described in Materials and Methods.<sup>41</sup> The kinetics of RecBC- and RecBCD-catalyzed unwinding of a 24-bp blunt-ended DNA [substrate I without the noncomplementary (dT)<sub>*n*</sub> tails] used in our previous studies<sup>42</sup> are shown in Fig. 3. Whereas RecBCD is able to initiate unwinding rapidly from a blunt DNA end, much less unwinding is catalyzed by RecBC. These single-turnover kinetic experiments were performed using

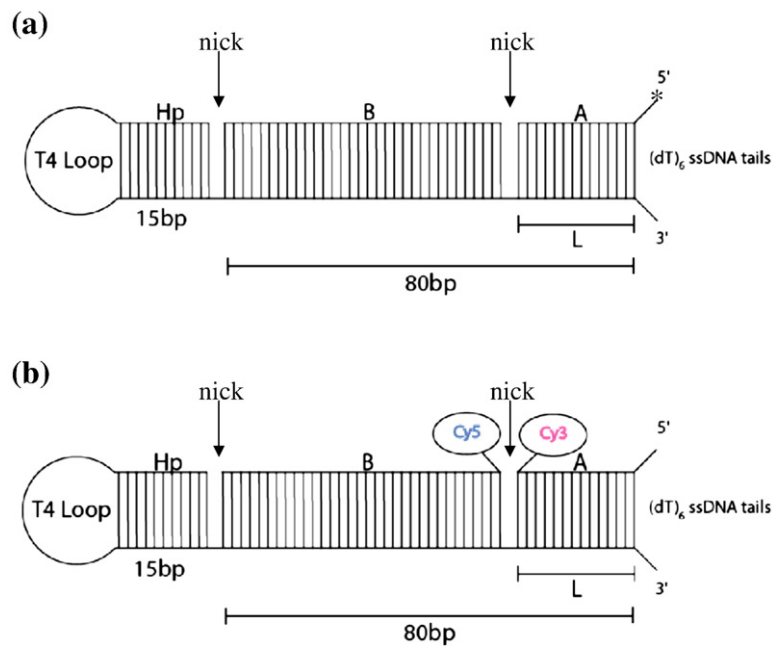


**Fig. 1.** Schematic representation of DNA substrates used in unwinding studies. Each DNA substrate is composed of three oligodeoxynucleotide strands, a constant bottom strand containing a hairpin (Hp) and two top strands—"A" and "B." These three DNA strands anneal to form a hairpin duplex containing two nicks. DNA substrates of different duplex lengths,  $L$ , are formed by varying the lengths of strands "A" and "B" while keeping their combined length constant. Because most substrates used in our unwinding studies possess noncomplementary ssDNA tails,  $L$  refers to the length of strand "A" that is base paired with the bottom strand and therefore must be unwound before DNA unwinding can be detected. (a) DNA substrates used in chemical quenched-flow unwinding experiments. Strand "A" is radiola-

beled with  $^{32}\text{P}$  at its 5' end (denoted by an asterisk), and the release of this strand is used to monitor DNA unwinding. (b) DNA substrates used in stopped-flow fluorescence measurements. A Cy3 and Cy5 FRET pair is positioned across a nick as depicted, and changes in FRET signal are used to monitor DNA unwinding.

the same preincubation concentration for RecBCD and RecBC (40 nM). We note that in a multiple-turnover experiment, our preparation of RecBC enzyme shows DNA unwinding behavior similar to that of a blunt-ended DNA substrate as reported

previously<sup>45</sup> (see Materials and Methods). One possibility is that the much lower amplitude of DNA unwinding by RecBC may result from a weaker affinity of RecBC for DNA blunt ends compared with RecBCD.<sup>37</sup> However, based on our

**Table 1.** Sequences of DNA unwinding substrates

DNA	Length (nt) <sup>a</sup>	DNA sequence
<i>Strand "A"</i>		
Ia	24	5'-(dT) <sub>n</sub> CCA TGG CTC CTG AGC TAG CTG CA(Cy3) G-3'
IIa	29	5'-(dT) <sub>n</sub> CCA TGG CTC CTG AGC TAG CTG CAG TAG C(Cy3)C-3'
IIIa	30	5'-(dT) <sub>n</sub> CCA TGG CTC CTG AGC TAG CTG CAG TAG CC(Cy3)T-3'
IVa	37	5'-(dT) <sub>n</sub> CCA TGG CTC CTGAGC TAG CTG CAG TAG CCT AAA GGA (Cy3)T-3'
Va	40	5'-(dT) <sub>n</sub> CCA TGG CTC CTG AGC TAG CTG CAG TAG CCT AAA GGA TGA C(Cy3)A-3'
VIa	43	5'-(dT) <sub>n</sub> CCA TGG CTC CTG AGC TAG CTG CAG TAG CCT AAA GGA TGA AAC (Cy3)T-3'
VIIa	48	5'-(dT) <sub>n</sub> CCA TGG CTC CTG AGC TAG CTG CAG TAG CCT AAA GGA TGA AAC TAG GA (Cy3)T-3'
VIIIa	53	5'-(dT) <sub>n</sub> CCA TGG CTC CTG AGC TAG CTG CAG TAG CCT AAA GGA TGA AAC TAG GAT CTT A(Cy3)T-3'
IXa	60	5'-(dT) <sub>n</sub> CCA TGG CTC CTG AGC TAG CTG CAG TAG CCT AAA GGA TGA AAC TAG GAT CTT ATG CTC CA(Cy3)T-3'
<i>Strand "B"</i>		
Ib	56	5'-(Cy5) TAG CCT AAA GGA TGA AAC TAG GAT CTT ATG CTC CAT GGA TAC GTC GAG TCG CAT CC-3'
IIb	51	5'-(Cy5) TAA AGG ATG AAA CTA GGA TCT TAT GCT CCA TGG ATA CGT CGA GTC GCA TCC-3'
IIIb	50	5'-(Cy5) AAA GGA TGA AAC TAG GAT CTT ATG CTC CAT GGA TAC GTC GAG TCG CAT CC-3'
IVb	43	5'-(Cy5) GAA ACT AGG ATC TTA TGC TCC ATG GAT ACG TCG AGT CGC ATC C-3'
Vb	40	5'-(Cy5) ACT AGG ATC TTA TGC TCC ATG GAT ACG TCG AGT CGC ATC C-3'
VIb	37	5'-(Cy5) AGG ATC TTA TGC TCC ATG GAT ACG TCG AGT CGC ATC C-3'
VIIb	32	5'-(Cy5) CTT ATG CTC CAT GCA TAC GTC GAG TCG CAT CC-3'
VIIIb	27	5'-(Cy5) GCT CCA TGG ATA CGT CGA GTC GCA TCC-3'
IXb	20	5'-(Cy5) GGA TAC GTC GAG TCG CAT CC-3'
<i>Strand Hp</i>		
Hp	120	5'-AGA TCC TAG TGC AGG TTT TCC TGC ACT AGG ATC TGG ATG CGA CTC GAC GTA TCC ATG GAG CAT AAG ATC CTA GTT TCA TCC TTT AGG CTA CTG CAG CTA GCT CAG GAG CCA TGG TTT TTT-3'

Substrate I is formed by annealing strand Ia, strand Ib, and the bottom strand Hp. Substrates II–IX are formed similarly. DNA strands "A" and "B" are fluorescently labeled with Cy3 and Cy5, respectively, for use in stopped-flow experiments.

<sup>a</sup> The length of DNA strand "A" refers to the number of base pairs that will form when annealed with the bottom strand (Hp) and therefore the DNA duplex length that is unwound in the kinetic experiment.

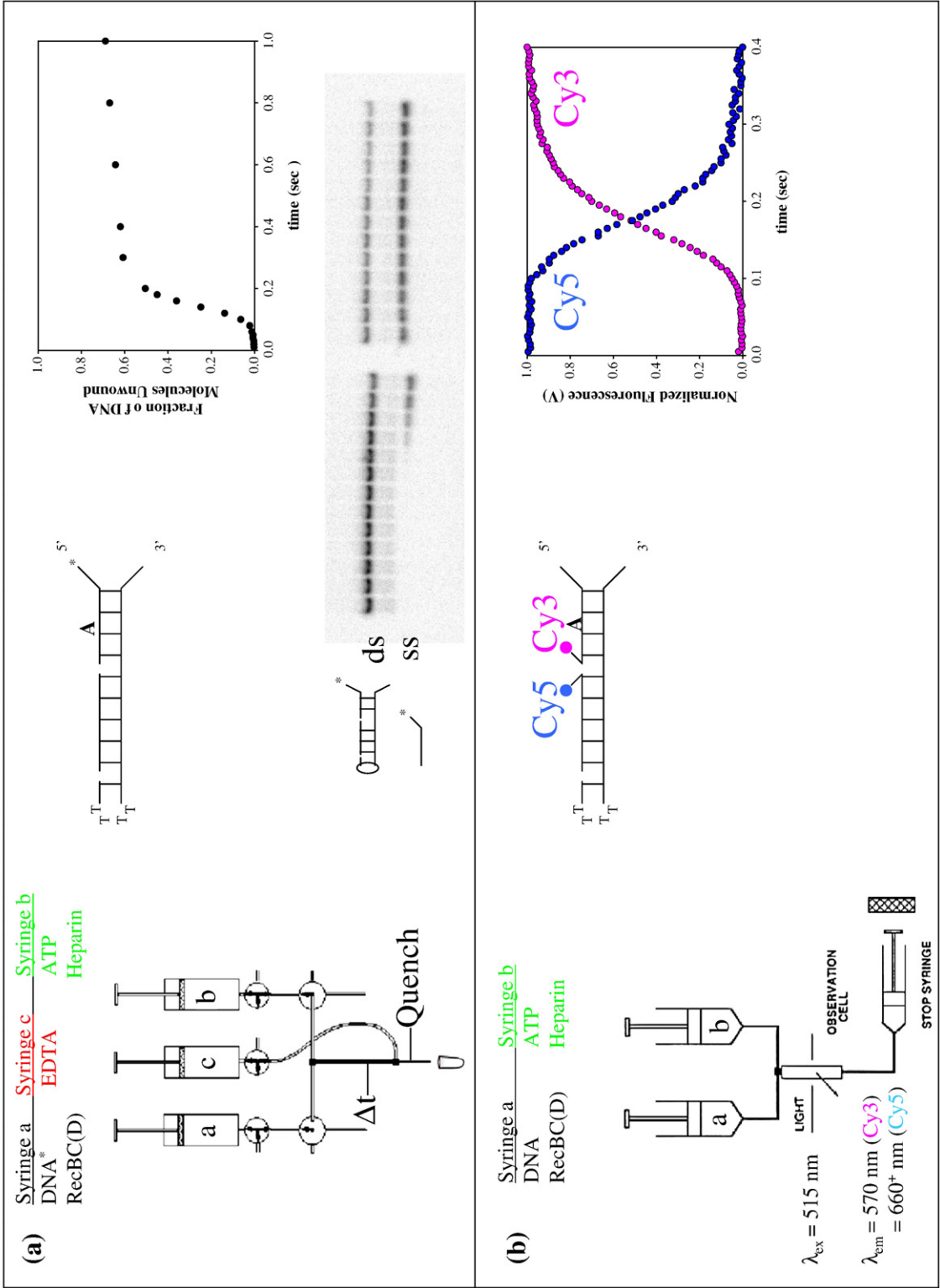
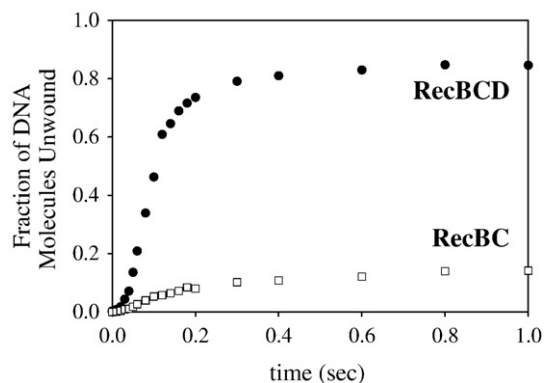


Fig. 2 (legend on next page)





**Fig. 3.** Comparison of the kinetics of DNA unwinding of a 24-bp blunt-ended DNA substrate (substrate I without noncomplementary dT tails) by RecBCD and RecBC. Single-turnover time courses, obtained using the quenched-flow assay, show that RecBCD (filled circles) initiates unwinding from a blunt DNA end with much higher efficiency than does RecBC (open squares).

estimate of  $2 \times 10^7 \text{ M}^{-1}$  for the equilibrium constant for RecBC binding to a blunt end under these conditions,<sup>37</sup> ~95% of the DNA ends should be bound with RecBC. Consistent with this conclusion, we observe no difference in the amplitude of unwinding when these experiments are performed using a 10-fold higher preincubation concentration (400 nM) of RecBC. This suggests that the majority of the RecBC enzyme must be bound in a nonproductive mode to a blunt duplex end. Previous studies have shown that RecBC binds with highest affinity to DNA ends possessing noncomplementary 5'-(dT)<sub>6</sub> and 3'-(dT)<sub>6</sub> ssDNA tails, while RecBCD binds optimally to DNA ends with noncomplementary 5'-(dT)<sub>10</sub> and 3'-(dT)<sub>6</sub> ssDNA tails.<sup>37</sup> Based on these, we examined the effect of such noncomplementary ssDNA tails on the kinetics and mechanism of DNA unwinding by both RecBC and RecBCD enzymes.

#### Minimal kinetic mechanism of RecBC-catalyzed DNA unwinding

We examined RecBC-catalyzed unwinding of a series of DNA duplexes possessing noncomplementary 5'-(dT)<sub>6</sub> and 3'-(dT)<sub>6</sub> ssDNA tails using rapid chemical quenched-flow and stopped-flow fluorescence techniques (see Materials and Methods).

Quenched-flow experiments were performed with DNA substrates of the type shown in Fig. 1a, with duplex region "A" varying in length [24, 30, 40, 48, and 60 bp (substrates I, III, V, VII, and XI, respectively)]. Three independent sets of measurements were performed with each duplex length. The average time courses are plotted in Fig. 4a and were analyzed by global nonlinear least-squares (NLLS) analysis using Scheme 1 (Eq. (2)). The continuous curves in Fig. 4a are simulated time courses using Eq. (2) and the best-fit parameters ( $m = 4.4 \pm 1.7 \text{ bp}$ ,  $k_{\text{obs}} = 90 \pm 25 \text{ s}^{-1}$ ;  $mk_{\text{obs}} = 396 \pm 15 \text{ bp/s}$ ,  $k_{\text{NP}} = 1.7 \pm 0.5 \text{ s}^{-1}$ ). It is clear from the data in Fig. 4a that RecBC is able to initiate DNA unwinding from a DNA end possessing the noncomplementary 5'-(dT)<sub>6</sub> and 3'-(dT)<sub>6</sub> ssDNA tails with much higher efficiency than from a blunt DNA end (see Fig. 3).

As observed previously for RecBCD-catalyzed unwinding of blunt-ended DNA duplexes, the time courses all display a lag phase. This lag phase results from the fact that the assays used are of the all-or-none type and RecBC must proceed through a series of sequential kinetic steps (with similar rate constants,  $k_U$ ) in order to fully unwind each duplex. The number of these unwinding steps, and thus the duration of the lag phase, increases with duplex length. In addition to this lag phase, we also observe a slower unwinding phase that is much smaller in amplitude. As discussed previously,<sup>41</sup> we attribute these two phases to DNA unwinding from two populations of initially bound RecBC–DNA complexes. One population of RecBC is bound in a productive mode that can initiate DNA unwinding rapidly upon the addition of ATP, while the other population of RecBC is bound in a nonproductive manner that must first undergo a slow isomerization, with rate constant  $k_{\text{NP}}$ , to form productive complexes before DNA unwinding can initiate.

Since RecBC-catalyzed unwinding of duplex DNA occurs via multiple ( $n$ ) repeated steps, with the rate-limiting rate constant,  $k_U$ , the number of DNA unwinding steps,  $n$ , is expected to increase in direct proportion to the DNA duplex length,  $L$ . In fact, Fig. 4b shows that the values of  $n$  determined from NLLS fitting of the data to the simple Scheme 1 are directly proportional to  $L$ . A summary of the kinetic parameters obtained from the NLLS fitting is given in Table 2. In Scheme 1, productively bound RecBC can unwind the DNA in uniform steps with rate con-

**Fig. 2.** Design of all-or-none chemical quenched-flow and stopped-flow fluorescence experiments to study single-turnover kinetics of DNA unwinding. (a) Quenched-flow assay. DNA substrates (radiolabeled with <sup>32</sup>P on the 5' end of strand "A") are incubated with excess RecBCD or RecBC helicase in one syringe. DNA unwinding is initiated by rapid mixing with ATP and heparin. The unwinding reaction is quenched after a time interval ( $\Delta t$ ) by rapid mixing with EDTA, and the ssDNA product produced after each time interval is separated from the native duplex DNA using nondenaturing PAGE and analyzed quantitatively after exposure to a phosphorimager (see Materials and Methods for details). (b) Stopped-flow assay. A DNA substrate labeled with donor (Cy3) and acceptor (Cy5) fluorophores as indicated is incubated with excess RecBCD or RecBC in one syringe, and DNA unwinding is initiated by rapid mixing with ATP and heparin. When Cy3 and Cy5 fluorophores are in close proximity, Cy3 fluorescence is decreased and Cy5 fluorescence is increased due to FRET. DNA unwinding is monitored in real time by the concomitant increase in Cy3 fluorescence and decrease in Cy5 fluorescence accompanying DNA unwinding and release of strand "A". Cy3 fluorescence is excited at 515 nm, and Cy3 fluorescence emission is monitored at 570 nm using an interference filter, while Cy5 fluorescence emission is monitored simultaneously at wavelengths above 665 nm using a long-pass filter.

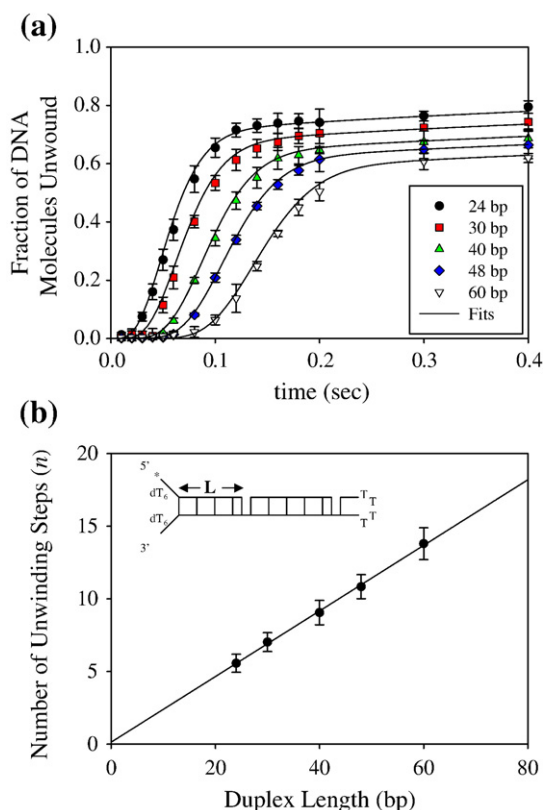


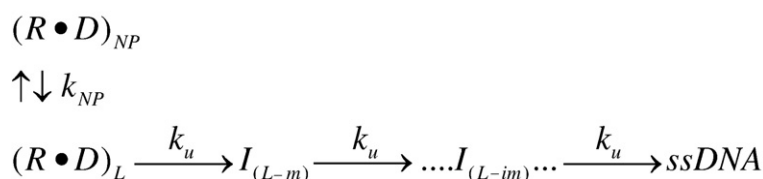
**Fig. 4.** Single-turnover kinetics of RecBC-catalyzed unwinding of DNA duplexes possessing noncomplementary 5'-(dT)<sub>6</sub> and 3'-(dT)<sub>6</sub> ssDNA tails. (a) Time courses as a function of duplex length [ $L=24$  bp (black circles);  $L=30$  bp (red squares);  $L=40$  bp (green triangles);  $L=48$  bp (blue diamonds);  $L=60$  bp (open inverted triangles)] obtained using the quenched-flow assay. Data points correspond to the average of three independent measurements, and the error bars indicate the standard deviation of the data. Smooth curves are simulated time courses based on the global NLLS best fits to Scheme 1, with  $mk_{\text{obs}}=396\pm15$  bp/s,  $m=4.4\pm1.7$  bp,  $k_{\text{obs}}=90\pm25$  s<sup>-1</sup>, and  $k_{\text{NP}}=1.7\pm0.5$  s<sup>-1</sup>. (b) The number of steps  $n$  determined from global NLLS analysis using Scheme 1 plotted versus DNA duplex length  $L$ . The continuous line shows the linear least-squares fit through the data ( $n=0.23L+0.03$ ).

tant  $k_{\text{U}}$ . The average kinetic step size,  $m$ , is defined as the average number of base pairs that are unwound between such two successive rate-limiting steps. Based on the NLLS fitting of the data in Fig. 4a, RecBC has an average kinetic step size of  $4.4\pm1.7$  bp for DNA unwinding, with a stepping rate of  $90\pm25$  s<sup>-1</sup>, resulting in a macroscopic unwinding rate  $mk_{\text{obs}}$  of  $396\pm15$  bp/s.

We also examined the kinetics of RecBC-catalyzed unwinding of DNA duplexes possessing noncomplementary twin 3'-(dT)<sub>6</sub> and 5'-(dT)<sub>6</sub> ssDNA tails using a stopped-flow fluorescence technique described previously.<sup>42</sup> These experiments were performed using a series of DNA substrates of the type shown in Fig. 1b, with duplex region “A” varying in length [24, 29, 37, 40, 43, 48, 53, and 60 bp (substrates I, II, IV, V, VI, VII, VIII, and IX, respectively)]. DNA unwinding was monitored by the loss of FRET between a Cy3 donor fluorophore and a Cy5 acceptor fluorophore. As indicated in Fig. 2b, the stopped-flow assay is also of the all-or-none type. When the DNA duplex is fully unwound and the labeled DNA strands are displaced, the two dyes become separated and thus Cy3 fluorescence increases, while there is a concomitant loss in Cy5 fluorescence due to the loss of energy transfer from Cy3 to Cy5.

The time courses monitoring the increase in Cy3 fluorescence (averages of three independent measurements) are plotted in Fig. 5a, and the continuous curves are global NLLS fits to the simple Scheme 1 (Eq. (2)) ( $m=4.4\pm0.1$  bp,  $k_{\text{obs}}=79\pm11$  s<sup>-1</sup>;  $mk_{\text{obs}}=348\pm5$  bp/s,  $k_{\text{NP}}=1.1\pm0.1$  s<sup>-1</sup>). These time courses are also well described by Scheme 1, and the number of unwinding steps,  $n$ , determined from the data fitting is directly proportional to duplex length,  $L$  (Fig. 5b). The Cy5 fluorescence time courses (see Supplementary Fig. 1), which are exactly anticorrelated with the Cy3 fluorescence time courses, can be analyzed as well using Scheme 1 (Eq. (2)), yielding identical kinetic parameters. It is interesting to note that in previous RecBCD stopped-flow unwinding studies,<sup>42</sup> the resulting Cy5 fluorescence time courses showed a more complex time course that was not fully anticorrelated with the Cy3 fluorescence time course. This deviation<sup>42</sup> was attributed to the RecD subunit, which translocates along the 5' ending DNA strand in the 5'-to-3' direction, ultimately contacting the Cy3 fluorophore at the nick, resulting in an enhancement of the Cy3 fluorescence. This increase in Cy3 fluorescence was then transferred via FRET to the Cy5 fluorophore before the strands are separated, resulting in an additional increase in Cy5 fluorescence. This effect is not observed with the RecBC enzyme because of the absence of the RecD translocating motor and since RecB translocates along the 3'-ended strand in the 3'-to-5' direction.

The advantage of the stopped-flow unwinding assay is that it is a continuous assay and thus many more time points can be obtained from a single experiment. As such, significantly more data



**Scheme 1.**

**Table 2.** Summary of chemical quenched-flow and stopped-flow fluorescence unwinding kinetic results

Quenched-flow results							
RecBCD	$mk_U$ (bp/s)	$k_U$ ( $s^{-1}$ )	$m$ (bp)	$k_C$ ( $s^{-1}$ )	$h$ (steps)	$k_{NP}$ ( $s^{-1}$ )	$x$
Blunt ends <sup>41</sup>	$790 \pm 23$	$196 \pm 77$	$3.9 \pm 1.3$	$29 \pm 3$	$2.0 \pm 0.2$	$1.1 \pm 0.2$	$0.84 \pm 0.02$
5'/3' T6	$774 \pm 16$	$240 \pm 56$	$3.3 \pm 1.3$	$45 \pm 2$	$3.2 \pm 0.2$	$1.1 \pm 0.3$	$0.89 \pm 0.04$
5' T10, 3' T6	$538 \pm 24$	$138 \pm 37$	$3.9 \pm 0.5$	–	0	$6.7 \pm 1.8$	$0.81 \pm 0.03$
Quenched-flow results							
RecBC	$mk_{obs}$ (bp/s)	$k_{obs}$ ( $s^{-1}$ )	$m$ (bp)	$k_C$ ( $s^{-1}$ )	$h$ (steps)	$k_{NP}$ ( $s^{-1}$ )	$x$
5'/3' T6	$396 \pm 15$	$90 \pm 25$	$4.4 \pm 1.7$	–	0	$1.7 \pm 0.5$	$0.81 \pm 0.02$
5' T10, 3' T6	$372 \pm 21$	$103 \pm 33$	$3.6 \pm 0.9$	–	0	$2.5 \pm 1.2$	$0.80 \pm 0.02$
Stopped-flow results							
RecBCD	$mk_U$ (bp/s)	$k_U$ ( $s^{-1}$ )	$m$ (bp)	$k_C$ ( $s^{-1}$ )	$h$ (steps)	$k_{NP}$ ( $s^{-1}$ )	$x$
Blunt ends <sup>46</sup>	$680 \pm 12$	$200 \pm 40$	$3.4 \pm 0.6$	$51 \pm 5$	$3.2 \pm 0.3$	$6.0 \pm 0.3$	$0.87 \pm 0.01$
5'/3' T6	$745 \pm 18$	$220 \pm 28$	$3.4 \pm 0.5$	$58 \pm 2$	$3.2 \pm 0.1$	$6.7 \pm 0.3$	$0.83 \pm 0.01$
5' T10, 3' T6	$588 \pm 11$	$163 \pm 24$	$3.6 \pm 0.2$	–	0	$5.4 \pm 1.0$	$0.80 \pm 0.01$
Stopped-flow results							
RecBC	$mk_{obs}$ (bp/s)	$k_{obs}$ ( $s^{-1}$ )	$m$ (bp)	$k_C$ ( $s^{-1}$ )	$h$ (steps)	$k_{NP}$ ( $s^{-1}$ )	$x$
5'/3' T6	$348 \pm 5$	$79 \pm 11$	$4.4 \pm 0.1$	–	0	$1.1 \pm 0.1$	$0.79 \pm 0.03$
5' T10, 3' T6	$320 \pm 7$	$92 \pm 12$	$3.5 \pm 0.1$	–	–	$1.9 \pm 0.6$	$0.81 \pm 0.02$

from many more duplex lengths can be analyzed, yielding better estimates of the kinetic parameters. However, since the quenched-flow experiment yields a direct measure of the extent of DNA

unwinding, we routinely perform and compare the results from both chemical quenched-flow and stopped-flow fluorescence studies. In this case, the kinetic parameters determined using both methods

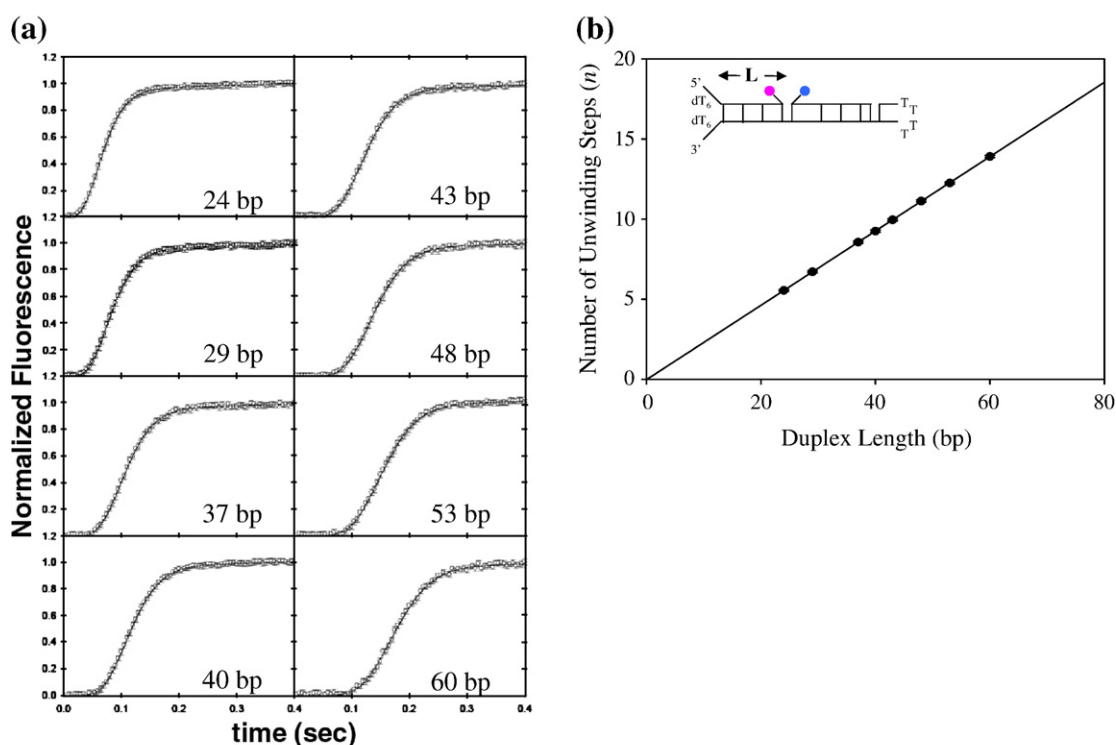


**Fig. 5.** Single-turnover kinetics of RecBC-catalyzed unwinding of DNA duplexes possessing noncomplementary 5'-(dT)<sub>6</sub> and 3'-(dT)<sub>6</sub> ssDNA tails using the stopped-flow fluorescence assay. (a) Cy3 fluorescence time courses as a function of duplex length ( $L = 24, 29, 37, 40, 43, 48, 53$ , and  $60$  bp). Data points represent the average of three independent measurements, and the error bars indicate the standard deviation of the data. Smooth curves are simulated time courses based on the global NLLS best fits to Scheme 1, with  $mk_{obs} = 348 \pm 5$  bp/s,  $m = 4.4 \pm 0.1$  bp,  $k_{obs} = 79 \pm 11$   $s^{-1}$ , and  $k_{NP} = 1.1 \pm 0.1$   $s^{-1}$ . (b) The number of unwinding steps  $n$  determined from the global NLLS analysis using Scheme 1 plotted versus DNA duplex length  $L$ . The continuous line shows the linear least-squares fit through the data ( $n = 0.23L - 0.02$ ).

are in good agreement, although some slight differences in the parameters are observed (see Table 2).

### RecBCD-catalyzed unwinding of DNA duplexes with twin (dT)<sub>6</sub> ssDNA tails

We next compared RecBC and RecBCD unwinding directly. However, since the previous RecBCD experiments examined DNA unwinding from blunt DNA ends,<sup>41,42</sup> we needed to examine RecBCD unwinding of duplexes possessing the noncomplementary twin (dT)<sub>6</sub> tails used in the RecBC studies. Figure 6a shows the time courses determined using the chemical quenched-flow assay (the time courses determined using the stopped-flow assay are shown in Supplementary Fig. 2a). The data in Fig. 6a were analyzed by global NLLS analysis using the simple Scheme 1 (Eq. (2)), and the continuous curves are time courses simulated using Eq. (2) and the best-fit parameters. Based on the poor quality of these fits,

Scheme 1 is not sufficient to describe these time courses. Consistent with this conclusion, Fig. 6b shows that a plot of the number of repeated rate-limiting kinetic steps,  $n$ , versus duplex length,  $L$ , exhibits a positive  $y$ -intercept. The fact that the fitted value of  $n$  is not directly proportional to  $L$  and that a positive  $y$ -intercept is observed suggest the presence of additional kinetic steps in the mechanism that are not directly associated with DNA unwinding.<sup>41,44</sup> As a result, we reanalyzed these time courses using the more complicated Scheme 2 (Eq. (4)), in which  $h$  additional kinetic steps with rate constant  $k_C$  are included in the mechanism, although these steps are not repeated within the series of DNA unwinding cycles. Scheme 2 is the same kinetic scheme that was used previously to analyze RecBCD-catalyzed unwinding of a series of blunt-ended DNA duplexes.<sup>41,42</sup> The time courses are well described by Scheme 2, as shown in Fig. 6c ( $m=3.3\pm1.3$  bp,  $k_U=240\pm56$  s<sup>-1</sup>;  $mk_U=774\pm16$  bp/s,  $h=3.2\pm0.2$ ,  $k_C=45\pm2$ ,  $k_{NP}=1.1\pm0.3$  s<sup>-1</sup>). Furthermore, after

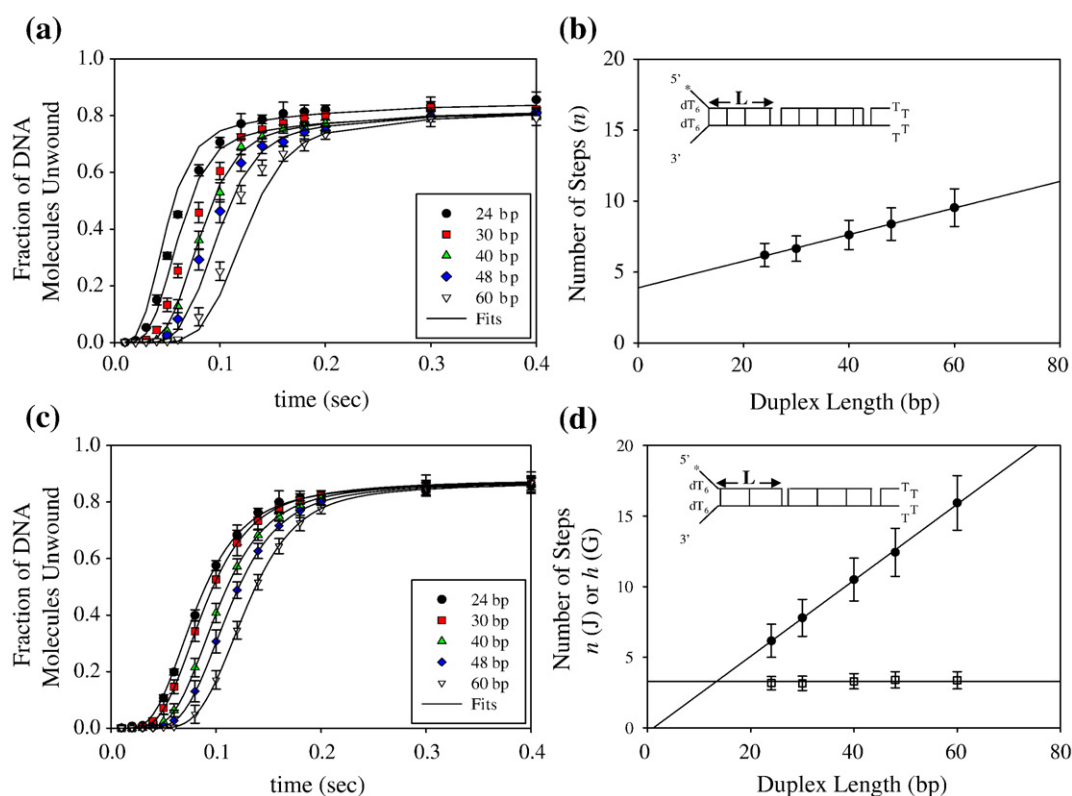
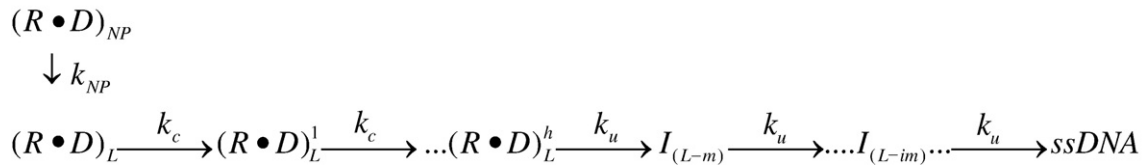


**Fig. 6.** Single-turnover kinetics of RecBCD-catalyzed unwinding of DNA duplexes possessing noncomplementary 5'-(dT)<sub>6</sub> and 3'-(dT)<sub>6</sub> ssDNA tails. (a) Time courses as a function of duplex length [ $L=24$  bp (black circles);  $L=30$  bp (red squares);  $L=40$  bp (green triangles);  $L=48$  bp (blue diamonds);  $L=60$  bp (open inverted triangles)] obtained using the quenched-flow assay. Data points correspond to the average of three independent measurements, and the error bars indicate the standard deviation of the data. Smooth curves are simulated time courses based on the global NLLS best fits to Scheme 1, with  $mk_U=410\pm12$  bp/s,  $m=10.1\pm0.9$  bp,  $k_U=39\pm23$  s<sup>-1</sup>, and  $k_{NP}=5.9\pm1.8$  s<sup>-1</sup>. (b) The number of steps  $n$  determined from global NLLS analysis using Scheme 1 plotted versus DNA duplex length  $L$ . The continuous line shows the linear least-squares fit through the data ( $n=0.09L+3.88$ ). (c) The same data from (a) were analyzed using Scheme 2, which includes the additional kinetic steps with rate constant  $k_C$ , which are not involved in DNA unwinding. Smooth curves are simulated time courses based on the global NLLS best fits to Scheme 2, with  $mk_U=774\pm16$  bp/s,  $m=3.3\pm1.3$  bp,  $k_U=240\pm56$  s<sup>-1</sup>,  $k_{NP}=1.1\pm0.3$  s<sup>-1</sup>,  $h=3.2\pm0.2$  steps, and  $k_C=45\pm2$  s<sup>-1</sup>. (d) The number of unwinding steps  $n$  and additional kinetic steps  $h$  determined from global NLLS analysis using Scheme 2 plotted versus DNA duplex length  $L$ . The continuous line shows the linear least-squares fit through the data ( $n=0.27L-0.21$ ;  $h=3.3$ ).





Scheme 2.

incorporating the additional  $k_c$  steps into the mechanism, the number of steps involved in unwinding,  $n$ , is found to be directly proportional to duplex length,  $L$ , while the number of additional steps,  $h$ , is independent of  $L$ , as shown in Fig. 6d. A summary of the kinetic parameters obtained from the fits of the quenched-flow and fluorescence time courses to Scheme 2 is given in Table 2.

### RecBCD-catalyzed unwinding of DNA possessing noncomplementary 5'-(dT)<sub>10</sub> and 3'-(dT)<sub>6</sub> ssDNA tails

Previous equilibrium binding experiments have shown that RecBCD binds optimally to DNA duplex ends possessing noncomplementary 5'-(dT)<sub>10</sub> and 3'-(dT)<sub>6</sub> ssDNA tails;<sup>37</sup> hence, we next examined RecBCD unwinding of DNA substrates possessing this DNA end structure under the same solution conditions used above. We first obtained time courses for five duplex lengths using the chemical quenched-flow unwinding assay. These time courses, shown in Fig. 7a, also display lag kinetics and are biphasic. Interestingly, in contrast to the time courses obtained with the DNA substrates possessing twin (dT)<sub>6</sub> ssDNA tails, these time courses are well described by the simple  $n$ -step sequential kinetic mechanism of Scheme 1 as shown by the continuous curves in Fig. 7a ( $m=3.9 \pm 0.5$  bp,  $k_U=138 \pm 37$  s<sup>-1</sup>;  $mk_U=538 \pm 24$  bp/s,  $k_{NP}=6.7 \pm 1.8$  s<sup>-1</sup>). Furthermore, Fig. 7b indicates that the number of steps involved in unwinding,  $n$ , is directly proportional to duplex length,  $L$ . The two to three additional steps, with rate constant  $k_c$ , that are part of Scheme 2 and required for RecBCD to initiate DNA unwinding from blunt ends and duplexes with twin (dT)<sub>6</sub> tails are not necessary to describe these time courses. This conclusion is also supported by time courses obtained for eight duplex lengths using the stopped-flow fluorescence assay (Supplementary Fig. 3a and b). Table 2 provides a summary of the kinetic parameters obtained from these experiments. RecBCD has the same average kinetic step size for unwinding ( $\sim 4$  bp) all three of the DNA molecules, independent of the end structure [blunt end, twin (dT)<sub>6</sub>, and 5'-(dT)<sub>10</sub> as well as 3'-(dT)<sub>6</sub>].

## Discussion

In previous studies of the mechanism of RecBCD-catalyzed unwinding of DNA using single-turnover methods, Lucius *et al.*<sup>40–42</sup> found that the time course

for RecBCD unwinding of blunt-ended DNA cannot be described by a simple sequential  $n$ -step kinetic model, such as that shown in Scheme 1. In fact, Scheme 2, which includes additional kinetic steps, was needed to describe the time courses for a range of duplex DNA lengths. The need to include these additional kinetic steps made it more difficult to

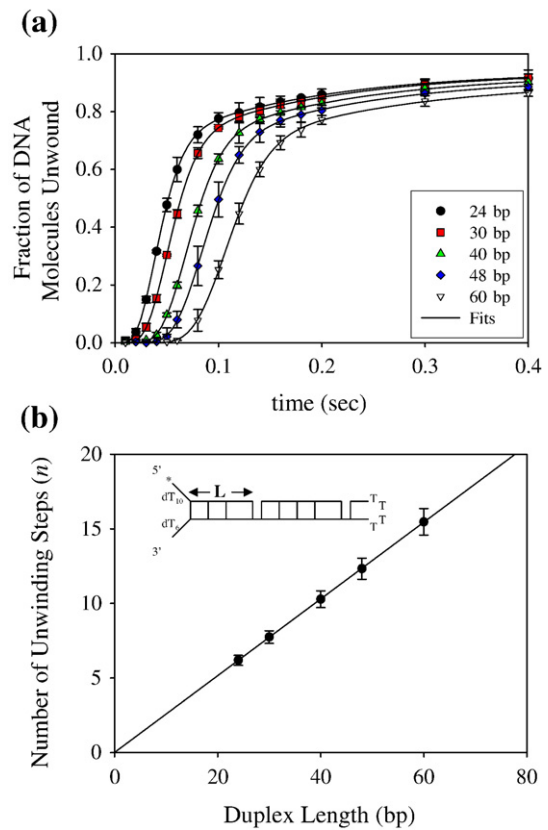


**Fig. 7.** Single-turnover kinetics of RecBCD-catalyzed unwinding of DNA duplexes possessing noncomplementary 5'-(dT)<sub>10</sub> and 3'-(dT)<sub>6</sub> ssDNA tails obtained. (a) Time courses obtained as a function of duplex length [ $L=24$  bp (black circles);  $L=30$  bp (red squares);  $L=40$  bp (green triangles);  $L=48$  bp (blue diamonds);  $L=60$  bp (open inverted triangles)] using the chemical quenched-flow assay. Data points represent the average of three independent measurements, and the error bars indicate the standard deviation of the data. Smooth curves are simulated time courses based on the global NLLS best fits to Scheme 1, with  $mk_U=538 \pm 24$  bp/s,  $m=3.9 \pm 0.5$  bp,  $k_U=138 \pm 37$  s<sup>-1</sup>, and  $k_{NP}=6.7 \pm 1.8$  s<sup>-1</sup>. (b) Plot of the number of unwinding steps  $n$  versus duplex length  $L$ . The continuous line shows the linear least-squares fit through the data ( $n=0.26L$ ).

estimate the DNA unwinding kinetic step size for RecBCD, although a well-constrained kinetic step size independent of ATP concentration and temperature of  $3.9 \pm 0.5$  bp was determined.<sup>40</sup> The number (two to three) of these additional steps with rate constant  $k_C$  was found to be independent of DNA duplex length; hence, these steps do not appear to be part of the repeated cycles of DNA unwinding and likely precede DNA unwinding.<sup>42</sup>

The experiments described in our current study show that these additional steps are still required for RecBCD to initiate unwinding from a duplex end possessing noncomplementary 5'-(dT)<sub>6</sub> and 3'-(dT)<sub>6</sub> ssDNA tails, yet they are not needed to describe the unwinding of DNA possessing a noncomplementary 5'-(dT)<sub>10</sub> tail in the presence of a 3'-(dT)<sub>6</sub> ssDNA tail. Interestingly, these additional steps are also not needed to describe the time course of RecBC-catalyzed unwinding of DNA duplexes possessing noncomplementary twin (dT)<sub>6</sub> ssDNA tails (Table 2). These results further support the conclusion that the additional  $k_C$  steps represent a real aspect of the mechanism for RecBCD initiation of DNA unwinding at a blunt-ended DNA. Furthermore, the less complex kinetic traces for RecBCD unwinding of duplex DNA possessing the noncomplementary 5'-(dT)<sub>10</sub> and 3'-(dT)<sub>6</sub> ssDNA tails are well described by the simple sequential  $n$ -step kinetic model (Scheme 1) and yield the same average kinetic step size ( $\sim 4$  bp) as previously reported for RecBCD unwinding of blunt-ended DNA, thus supporting the previous analyses.<sup>40–42</sup>

### Functional significance of the additional $k_C$ steps

The results from the current study, along with recent DNA binding<sup>37</sup> and structural<sup>39</sup> studies, suggest a role for these additional kinetic steps with rate constant  $k_C$ . A crystal structure of RecBCD bound to a blunt-ended duplex shows 4 bp melted from the blunt end within the complex;<sup>39</sup> however, the 4 nt that are not base paired on the 5' ssDNA end do not contact any part of the RecD subunit. Equilibrium DNA binding studies<sup>37</sup> suggest that a 5' ssDNA tail of at least 10 nt [(dT)<sub>10</sub>] is needed to make full contact with the RecD subunit within the RecBCD–DNA complex. Computer modeling studies also suggest that extension of the 5' ssDNA tail to 10 nt is needed to contact the RecD subunit.<sup>47</sup> These findings suggest that the additional  $k_C$  steps that are required to describe RecBCD-catalyzed unwinding from a blunt-ended DNA duplex or a DNA duplex possessing twin (dT)<sub>6</sub> ssDNA tails reflect the process of initiating binding of the RecD subunit with the 5' ssDNA tail. This might involve pausing or molecular rearrangement steps that take place after the 5' ssDNA end becomes sufficient in length to reach RecD, thereby enabling this subunit to initiate DNA unwinding. In this scenario, upon ATP binding and hydrolysis, the RecB motor in the RecBCD–DNA complex acting on the 3' ssDNA strand would begin to unwind the duplex and translocate along the

DNA until it creates a 5' ssDNA tail long enough, at least 10 nt, so that RecD can interact with the 5' ssDNA strand and initiate translocation. Studies of the RecB<sup>K29Q</sup>CD protein, where the RecB motor is inactivated via a mutation in the ATP binding site,<sup>48</sup> showed that a 4-nt 5' ssDNA tail on the DNA end is required for DNA unwinding. This observation is consistent with our results since upon melting of the 6 bp at the duplex DNA end, this would yield a 10-nt-long 5' ssDNA tail, which would allow interaction of RecD.

Interestingly, although the additional  $k_C$  steps are not needed to describe RecBCD unwinding of duplex DNA possessing noncomplementary 5'-(dT)<sub>10</sub> and 3'-(dT)<sub>6</sub> ssDNA tails, the macroscopic rate of DNA unwinding that we estimate is slightly slower ( $538 \pm 24$  bp s<sup>-1</sup>) than that for RecBCD unwinding of a blunt-ended DNA ( $790 \pm 23$  bp s<sup>-1</sup>) or a duplex DNA possessing noncomplementary twin (dT)<sub>6</sub> tails ( $774 \pm 16$  bp s<sup>-1</sup>). Currently, we cannot explain this slower observed rate of DNA unwinding. However, it has recently been shown that the rate of RecBCD unwinding becomes slower after RecBCD interacts with a “chi” sequence in the unwound ssDNA due to a switching of the lead motor from RecD to RecB.<sup>23</sup> In light of this, it is possible that when RecBCD initiates unwinding from a blunt-ended DNA or a duplex end possessing noncomplementary 3'-(dT)<sub>6</sub> and 5'-(dT)<sub>6</sub> tails, it starts in a “pre-chi” state with a faster rate. However, when RecBCD initiates unwinding from a duplex end possessing an extended 5' ssDNA tail of 10 nt, it may initiate unwinding as if it were in a “post-chi” state. Further experiments will be needed to test this hypothesis.

We note that there is a potential ambiguity in the analyses of the experiments reported here, specifically with regard to the actual length of duplex DNA that should be considered unwound by RecBCD or RecBC during its ATP-dependent unwinding (helicase) reaction. We find that the kinetic parameters determined for RecBCD unwinding of a series of blunt-ended DNA duplexes varying in length,  $L$  (bp), are identical within experimental error with the kinetic parameters determined for RecBCD unwinding of a series of DNA duplexes possessing noncomplementary 5'- and 3'-(dT)<sub>6</sub> tails. However, when RecBCD forms an initiation complex with a blunt duplex DNA end, the enzyme can melt out 5–6 bp in a Mg<sup>2+</sup>- or Ca<sup>2+</sup>-dependent reaction;<sup>37–39</sup> hence, the effective duplex length with prebound RecBCD is potentially  $\sim 5$ –6 bp shorter than the actual length of the duplex region. Yet, when RecBCD binds to a DNA end possessing noncomplementary twin (dT)<sub>6</sub> ssDNA tails or 5'-(dT)<sub>10</sub> and 3'-(dT)<sub>6</sub> ssDNA tails, no additional base pair melting presumably occurs.<sup>37</sup> This becomes an issue when we relate the number of kinetic steps,  $n$ , determined from the NLLS analysis to the length of the duplex DNA that is unwound, which in turn would potentially affect the estimation of the kinetic step size,  $m$ . In an attempt to assess the effects of this ambiguity, we reanalyzed the time courses for RecBCD-catalyzed unwinding of blunt-ended DNA

in two ways. We assumed that each DNA duplex length is actually  $(L-6)$  bp rather than  $L$  bp when RecBCD is initially bound to the blunt-ended DNA but before unwinding is initiated. We then compared the plots of  $n$  versus  $(L-6)$  and  $n$  versus  $L$  for the blunt-ended duplexes with the plot of  $n$  versus  $L$  for RecBCD unwinding of the twin  $(dT)_6$ -tailed DNA substrate. We find that the kinetic parameters determined from these three analyses are identical within our experimental uncertainty; hence, this potential ambiguity has no influence on the kinetic parameters that we report here. On the other hand, even though RecBCD melts out 5–6 bp upon binding to a blunt DNA end, the enzyme may still need to proceed through the same number,  $n$ , of repeated rate-limiting steps to fully unwind a blunt-ended DNA of duplex length,  $L$ , or a DNA with duplex length  $(L-6)$  bp that possesses noncomplementary twin  $(dT)_6$  tails. This could result if the  $n$  repeated rate-limiting kinetic steps are not associated with the actual DNA unwinding process, which may be much faster, but with a slower process (e.g., a protein conformational change) that is repeated every  $\sim 4$  bp (on average) during the unwinding cycle. Hence, even if 5–6 bp of a duplex end are premelted, the “kinetic step” may not be complete until it proceeds through the rate-limiting step and thus the total number of rate-limiting steps needed to fully unwind the DNA could be unchanged.

### RecBC and RecBCD display the same average kinetic step size for DNA unwinding

We have shown that RecBC initiates DNA unwinding poorly from a blunt DNA end and that its ability to initiate unwinding is greatly enhanced when RecBC is prebound to a duplex possessing noncomplementary twin  $(dT)_6$  ssDNA tails. We have recently shown that RecBC appears to be able to melt out at least 4 bp upon binding to a blunt DNA duplex end in a  $Mg^{2+}$ -dependent but ATP-independent reaction,<sup>46</sup> similar to the reaction demonstrated for RecBCD.<sup>38</sup> However, the kinetic results reported here suggest that the complex formed by RecBC upon binding to a blunt DNA end must differ in some important functional manner from the RecBCD complex. Yet, once initiated, RecBC unwinds DNA with an average kinetic step size of  $\sim 4$  bp, which is the same as the average kinetic step size for RecBCD unwinding. RecBC unwinding studies performed as a function ATP concentration (C. Wu and T. M. Lohman, unpublished data) indicate that this average kinetic step size is also independent of ATP concentration, as observed previously for RecBCD.<sup>40</sup> These data suggest that the same rate-limiting kinetic process is repeated every  $\sim 4$  bp on average during DNA unwinding by both RecBCD and RecBC, although the rate of this process is slower for RecBC.

It is not clear how the kinetic step size measured in our single-turnover ensemble studies may relate to a mechanical step size, as measured in a single-molecule experiment. However, it is worth noting that these should only be the same if the process that

limits the rate of DNA unwinding is the same as the process that limits the rate of the mechanical step. For example, Bianco and Kowalczykowski<sup>45</sup> proposed a “quantum-inch worm model” for RecBC unwinding and translocation based on the observation that RecBC is able to bypass flexible ssDNA gaps in duplex DNA as large as  $\sim 23$  nt. In this model, the enzyme is viewed as having two DNA binding sites such that DNA unwinding occurs in a series of small steps of a few base pairs, whereas larger translocation steps of  $\sim 23$  bp can also occur. In this model, the unwinding step size could be smaller than the translocation step size. Based on the experiments reported here, we observe a smaller ( $\sim 4$  bp) kinetic step size for RecBC unwinding. However, if translocation and unwinding occur with different step sizes, the relative rates of the steps limiting unwinding versus translocation would determine which step is observed in a measurement of a kinetic step size. Previous single-molecule studies of RecBCD unwinding<sup>49</sup> were unable to resolve individual steps, although those experiments placed an upper limit for the step size of a few base pairs.

## Materials and Methods

### Buffers and reagents

Buffers were prepared with reagent-grade chemicals and doubly distilled water that was deionized further using a Milli-Q purification system (Millipore Corp., Bedford, MA). All buffers and reagents were filtered using  $0.2\text{-}\mu\text{m}$  filters after preparation. RecBCD storage buffer is buffer C: 20 mM  $KP_i$ , pH 6.8 at 25 °C, 0.1 mM 2-mercaptoethanol, 0.1 mM ethylenediaminetetraacetic acid (EDTA), and 10% (v/v) glycerol. DNA unwinding reaction buffer is buffer M: 20 mM Mops-KOH, pH 7.0 at 25 °C, 30 mM NaCl, 10 mM  $MgCl_2$ , 1 mM 2-mercaptoethanol, and 5% (v/v) glycerol.

Heparin stock solutions were prepared by dissolving heparin sodium salt (lot no. 114K1328; Sigma, St. Louis, MO) in buffer M and dialyzing it further against buffer M using a 3500-molecular-weight-cutoff dialysis tubing. Heparin stock concentrations were determined by titration with Azure A as described previously<sup>50</sup> and stored at 4 °C until use.

ATP stock solutions were prepared by dissolving adenosine 5'-triphosphate sodium salt (lot no. 016K7008; Sigma) in water and adjusting the pH to 7.0 with NaOH. Stock aliquots were stored at  $-20$  °C until use, and stock concentrations were determined spectrophotometrically using an extinction coefficient of  $\epsilon_{260} = 1.5 \times 10^4 \text{ M}^{-1} \text{ cm}^{-1}$ .<sup>51</sup>

### Proteins

*E. coli* RecB and RecC were purified and stored in buffer C at  $-80$  °C as described previously.<sup>41,42</sup> The RecBC enzyme was reconstituted by mixing equimolar RecB and RecC on ice. RecBC was dialyzed against buffer M at 4 °C before use, and its concentration was determined spectrophotometrically using an extinction coefficient of  $\epsilon_{280} = 3.9 \times 10^5 \text{ M}^{-1} \text{ cm}^{-1}$ .<sup>37</sup> We have examined and compared our RecBC preparation with RecBC that was purified from *E. coli* directly as the heterodimer [kindly



provided by A. Taylor and G. Smith (Fred Hutchinson Cancer Center, Seattle, WA)] and observed no difference between the two preparations with respect to DNA binding<sup>37</sup> and single-turnover DNA unwinding. On the other hand, in multiple-turnover experiments, Bianco and Kowalczykowski<sup>45</sup> observed that ~65% of a blunt-ended DNA substrate is unwound after 2 min. For comparison, we also performed multiple-turnover unwinding experiments with a 24-bp blunt-ended DNA substrate [substrate I without the noncomplementary (dT)<sub>n</sub> tails] under the same solution conditions used in that study<sup>45</sup> and observed similar results (~56% unwinding after 2 min).

*E. coli* RecBCD was purified as a heterotrimer and stored in buffer C at -80 °C as described previously.<sup>36,41,52,53</sup> RecBCD was dialyzed against buffer M at 4 °C before use, and its concentration was determined spectrophotometrically using an extinction coefficient of  $\epsilon_{280} = 4.5 \times 10^5 \text{ M}^{-1} \text{ cm}^{-1}$ .<sup>36,41,52,53</sup> Dialyzed RecBCD and RecBC were used immediately (within 1 day) since a loss of activity (5%–15%) occurred after 5 days at 4 °C in buffer M.<sup>36,37,41,52,53</sup>

Bovine serum albumin (BSA) was purchased from Roche (Indianapolis, IN) and dialyzed against buffer M at 4 °C. Dialyzed BSA stock was stored at 4 °C until use, and stock concentration was determined spectrophotometrically using an extinction coefficient of  $\epsilon_{280} = 4.3 \times 10^4 \text{ M}^{-1} \text{ cm}^{-1}$ .<sup>37,54</sup>

### Oligodeoxynucleotides

Oligodeoxynucleotides were synthesized using an ABI model 391 synthesizer (Applied Biosystems, Foster City, CA) as described previously.<sup>55</sup> Unlabeled DNA was purified using PAGE under denaturing conditions followed by gel electroelution, while Cy3- and Cy5-labeled DNA was further purified by reversed-phase HPLC using an XTerra MS C18 column (Waters, Milford, MA).<sup>55</sup> The concentrations of each stock of DNA strands were determined by digesting each strand with phosphodiesterase I (Worthington, Lakewood, NJ) in 100 mM Tris-HCl, pH 9.2 at 25 °C, and 3 mM MgCl<sub>2</sub> and analyzing the resulting mixture of mononucleotides spectrophotometrically using the following extinction coefficients:<sup>51</sup>  $\epsilon_{260, \text{AMP}} = 15,340 \text{ M}^{-1} \text{ cm}^{-1}$ ,  $\epsilon_{260, \text{CMP}} = 7600 \text{ M}^{-1} \text{ cm}^{-1}$ ,  $\epsilon_{260, \text{GMP}} = 12,160 \text{ M}^{-1} \text{ cm}^{-1}$ ,  $\epsilon_{260, \text{TMP}} = 8700 \text{ M}^{-1} \text{ cm}^{-1}$ ,  $\epsilon_{260, \text{Cy3}} = 5000 \text{ M}^{-1} \text{ cm}^{-1}$ , and  $\epsilon_{260, \text{Cy5}} = 10,000 \text{ M}^{-1} \text{ cm}^{-1}$ .

### DNA substrate design

The DNA substrates used for DNA unwinding studies were composed of three DNA strands that form a hairpin structure when annealed together with the exception of two nicks as shown in Fig. 1.<sup>36,41,42</sup> For chemical quenched-flow experiments, strand "A" was radiolabeled on its 5' end as depicted in Fig. 1a with <sup>32</sup>P using T4 polynucleotide kinase (USB, Cleveland, OH) and  $\gamma$ -<sup>32</sup>P-ATP (Perkin Elmer, Waltham, MA) as described previously.<sup>55</sup> The radiolabeled strand "A" was mixed with an equal molar ratio of strand "B" and 25% excess of the bottom strand. The resulting DNA stock solution was heated to 94 °C for 5 min, followed by slow cooling to 25 °C to allow annealing. For stopped-flow unwinding experiments, strand "A" was fluorescently labeled with a Cy3 donor, while strand "B" was labeled with a Cy5 acceptor as depicted in Fig. 1b. These two fluorescently labeled DNA strands were mixed and annealed to the bottom strand as described above.

### Rapid chemical quenched-flow DNA unwinding kinetics

DNA unwinding experiments were performed at 25 °C using a quenched-flow apparatus (KinTek RQF-3, University Park, PA) as described previously.<sup>41</sup> RecBCD or RecBC (20 nM) was preincubated with <sup>32</sup>P-labeled DNA substrate (2 nM) and BSA (6  $\mu$ M) on ice for 20 min in buffer M, and this mixture was then loaded into one loop of the quenched-flow apparatus. Equilibrium binding experiments indicate that all unwinding substrates were saturated under these solution conditions and at these protein and DNA concentrations.<sup>37</sup> A solution containing ATP (10 mM) and heparin trap (15 mg/ml) in buffer M was loaded into the other loop. After equilibration at 25 °C for 5 min, DNA unwinding was initiated by rapidly mixing these solutions together (1:1) and quenching the reaction after a predefined time interval ( $\Delta t$ ) by mixing with 0.4 M EDTA and 10% (v/v) glycerol; the zero time point was determined by performing a "mock reaction" (without ATP). Quenched reactions collected at each time point were kept on ice until all samples were collected, and the unwound ssDNA was separated from the native duplex DNA using nondenaturing [10% (w/v)] PAGE. The gel was exposed to a phosphor screen (Molecular Dynamics, Sunnyvale, CA) for 1 h, after which the screen was scanned using a Storm 840 phosphorimager (Molecular Dynamics). The radioactivity of each band was quantified using the ImageQuant software (Molecular Dynamics), and the fraction of DNA molecules unwound at each time point,  $f_{ss}(t)$ , was calculated using Eq. (1):<sup>41</sup>

$$f_{ss}(t) = \frac{\frac{C_S(t)}{C_S(t) + C_D(t)} - \frac{C_{S,0}}{C_{S,0} + C_{D,0}}}{1 - \frac{C_{S,0}}{C_{S,0} + C_{D,0}}} \quad (1)$$

where  $C_S(t)$  and  $C_D(t)$  reflect the radioactive counts for the unwound ssDNA and the native duplex DNA, respectively, at time  $t$ , while  $C_{S,0}$  and  $C_{D,0}$  represent the corresponding quantities at time zero. Unwinding time courses were collected as a function of duplex length ( $L = 24, 30, 40, 48$ , and 60 bp), and the averages of three independent unwinding time courses for each duplex length were subjected to global NLLS analysis.

### Stopped-flow fluorescence unwinding kinetics

Fluorescence DNA unwinding experiments were performed at 25 °C using a stopped-flow apparatus (SX.18MV, Applied Photophysics Ltd., Leatherhead, UK) as described previously.<sup>40,42</sup> RecBC or RecBCD (200 nM) was preincubated with each Cy3- and Cy5-labeled DNA substrate (40 nM) and BSA (6  $\mu$ M) on ice for 20 min in buffer M. Equilibrium binding experiments indicate that all unwinding substrates were saturated under these solution conditions and at these protein and DNA concentrations.<sup>37</sup> This mixture was then loaded into one syringe of the stopped-flow apparatus, and a solution containing ATP (10 mM) and heparin (15 mg/ml) in buffer M was loaded into the other syringe of the device. Both solutions were equilibrated to 25 °C for 5 min, after which DNA unwinding was initiated by rapid mixing of the two solutions (1:1). The Cy3 fluorophore was excited at 515 nm, and its emission was monitored at 570 nm with an interference filter (Oriol Corp., Stratford, CT); Cy5 emission was monitored simultaneously at all wavelengths >665 nm using a long-pass filter (Oriol Corp.). Ten individual Cy3 FRET time courses were collected and



averaged, and unwinding experiments were performed as a function of duplex length ( $L=24, 29, 37, 40, 43, 48, 53$ , and  $60$  bp). The results from three independent measurements were averaged and subjected to global NLLS analysis. Since all Cy3 FRET time courses exhibit a lag phase before fluorescence enhancement, this initial signal was assumed to represent 100% duplex DNA and thus reflect zero DNA unwinding. Hence, the first 10 data points from each time course were averaged and subtracted from all data points, thereby constraining each time course to start at zero.<sup>42</sup>

### Analysis of DNA unwinding kinetics

Global NLLS analysis of DNA unwinding kinetics was performed as described previously<sup>41,42,44</sup> using Conlin<sup>56</sup> (kindly provided by Dr. Jeremy Williams and modified by Dr. Chris Fischer) and IMSL C Numerical Libraries (Visual Numeric Incorporated, Houston, TX). The uncertainties reported reflect 68% confidence interval limits determined from a 50-cycle Monte Carlo analysis as described previously.<sup>41</sup> Entire time courses with data collected out to 10 s were used in the analysis, although only data out to 0.4 s were plotted here for clarity. Fitting of the time courses to a particular kinetic scheme was performed by obtaining the time-dependent formation of ssDNA,  $f_{ss}(t)$ , as the inverse Laplace transform of  $F_{ss}(s)$  using numerical methods as described previously.<sup>41,44</sup> For Scheme 1,  $f_{ss}(t)$  is given by Eq. (2):

$$\begin{aligned} f_{ss}(t) &= A_T \mathcal{L}^{-1} F_{ss}(s) \\ &= A_T \mathcal{L}^{-1} \left( \frac{k_U^n (k_{NP} + sx)}{s(k_{NP} + s)(k_U + s)^n} \right) \end{aligned} \quad (2)$$

where  $F_{ss}(s)$  is the Laplace transform of  $f_{ss}(t)$ ,  $\mathcal{L}^{-1}$  is the inverse Laplace transform operator with  $s$  as the Laplace variable,  $A_T$  is the total amplitude for a given duplex length  $L$ ,  $n$  is the number of unwinding steps with  $k_U$  being the rate constant in between two successive unwinding steps,  $k_{NP}$  is the rate constant for the isomerization reaction from nonproductive,  $(RD)_{NP}$  to productive,  $(RD)_L$ , RecBC(D)-DNA complexes, and  $x$  is the fraction of productively bound RecBC(D)-DNA complexes defined by Eq. (3):

$$x = \frac{(RD)_L}{(RD)_L + (RD)_{NP}} \quad (3)$$

$f_{ss}(t)$  for Scheme 2 is given by Eq. (4) in which  $h$  additional kinetic steps with rate constant  $k_C$  that are not directly associated with DNA unwinding have been included in the mechanism:

$$\begin{aligned} f_{ss}(t) &= A_T \mathcal{L}^{-1} F_{ss}(s) \\ &= A_T \mathcal{L}^{-1} \left( \frac{k_C^h k_U^n (k_{NP} + sx)}{s(k_C + s)^h (k_{NP} + s)(k_U + s)^n} \right) \end{aligned} \quad (4)$$

In Figs. 4b–7b,  $A_T$ ,  $n$ ,  $h$  (where appropriate), and  $x$  were allowed to float for each duplex length, while  $k_C$  (where appropriate),  $k_U$ , and  $k_{NP}$  were constrained to be global parameters. In Figs. 4a–7a,  $n$  in Eqs. (2) and (4) was replaced with  $L/m$ , where  $L$  is duplex length in base pairs and  $m$  is the average unwinding kinetic step size. In this analysis,  $A_T$  and  $x$  (as well as  $h$ , where appropriate) were floated for each time course at every duplex length, while

$k_U$ ,  $k_{NP}$ , and  $m$  (as well as  $k_C$ , where appropriate) were constrained to be global parameters.

### Acknowledgements

This work was supported in part by the National Institutes of Health through grant GM045948. We thank Thang Ho for synthesis and purification of all DNA substrates; Drs. Gerald Smith and Doug Julin for providing plasmids and cell lines; and Drs. Aaron Lucius, Anita Niedziela-Majka, Jason Wong, and Tom Perkins for valuable discussions.

### Supplementary Data

Supplementary data associated with this article can be found, in the online version, at [doi:10.1016/j.jmb.2008.07.012](https://doi.org/10.1016/j.jmb.2008.07.012)

### References

1. Lohman, T. M. & Bjornson, K. P. (1996). Mechanisms of helicase-catalyzed DNA unwinding. *Annu. Rev. Biochem.* **65**, 169–214.
2. Lohman, T. M., Hsieh, J., Maluf, N. K., Cheng, W., Lucius, A. L., Fischer, C. J. *et al.* (2003). DNA helicases, motors that move along nucleic acids: lessons from the SF1 helicase superfamily. In *The Enzymes* (Tamanai, F. & Hackney, D. D., eds), vol. XXIII, pp. 303–369, Academic Press, New York, NY.
3. Matson, S. W., Bean, D. W. & George, J. W. (1994). DNA helicases: enzymes with essential roles in all aspects of DNA metabolism. *BioEssays*, **16**, 13–22.
4. Patel, S. S. & Donmez, I. (2006). Mechanisms of helicases. *J. Biol. Chem.* **281**, 18265–18268.
5. Patel, S. S. & Picha, K. M. (2000). Structure and function of hexameric helicases. *Annu. Rev. Biochem.* **69**, 651–697.
6. Delagoutte, E. & von Hippel, P. H. (2002). Helicase mechanisms and the coupling of helicases within macromolecular machines: Part I. Structures and properties of isolated helicases. *Q. Rev. Biophys.* **35**, 431–478.
7. Singleton, M. R., Dillingham, M. S. & Wigley, D. B. (2007). Structure and mechanism of helicases and nucleic acid translocases. *Annu. Rev. Biochem.* **76**, 23–50.
8. Flores, M. J., Sanchez, N. & Michel, B. (2005). A fork-clearing role for UvrD. *Mol. Microbiol.* **57**, 1664–1675.
9. Jankowsky, E., Gross, C. H., Shuman, S. & Pyle, A. M. (2001). Active disruption of an RNA–protein interaction by a DEXH/D RNA helicase. *Science*, **291**, 121–125.
10. Veaute, X., Delmas, S., Selva, M., Jeusset, J., Le Cam, E., Matic, I. *et al.* (2005). UvrD helicase, unlike Rep helicase, dismantles RecA nucleoprotein filaments in *Escherichia coli*. *EMBO J.* **24**, 180–189.
11. Eggleston, A. K., O'Neill, T. O., Bradbury, E. M. & Kowalczykowski, S. C. (1995). Unwinding of nucleosomal DNA by a DNA helicase. *J. Biol. Chem.* **270**, 2024–2031.
12. Byrd, A. K. & Raney, K. D. (2006). Displacement of a

- DNA binding protein by Dda helicase. *Nucleic Acids Res.* **34**, 3020–3029.
13. German, J., Sanz, M. M., Ciocchi, S., Ye, T. Z. & Ellis, N. A. (2007). Syndrome-causing mutations of the BLM gene in persons in the Bloom's Syndrome Registry. *Hum. Mutat.* **28**, 743–753.
  14. Ellis, N. A., Groden, J., Ye, T.-Z., Straughen, J., Lennon, D., Ciocchi, J. *et al.* (1995). The Bloom's syndrome gene product is homologous to RecQ helicases. *Cell*, **83**, 655–666.
  15. Hickson, I. D., Davies, S. L., Li, J. L., Levitt, N. C., Mohaghegh, P., North, P. S. & Wu, L. (2001). Role of the Bloom's syndrome helicase in maintenance of genome stability. *Biochem. Soc. Trans.* **29**, 201–204.
  16. Hickson, I. D. (2003). RecQ helicases: caretakers of the genome. *Nat. Rev. Cancer*, **3**, 169–178.
  17. Finch, P. W., Storey, A., Brown, K., Hickson, I. D. & Emmerson, P. T. (1986). Complete nucleotide sequence of *recD*, the structural gene for the  $\alpha$  subunit of exonuclease V of *Escherichia coli*. *Nucleic Acids Res.* **14**, 8583–8594.
  18. Finch, P. W., Storey, A., Chapman, K. E., Brown, K., Hickson, I. D. & Emmerson, P. T. (1986). Complete nucleotide sequence of the *Escherichia coli recB* gene. *Nucleic Acids Res.* **14**, 8573–8582.
  19. Finch, P. W., Wilson, R. E., Brown, K., Hickson, I. D., Tomkinson, A. E. & Emmerson, P. T. (1986). Complete nucleotide sequence of the *Escherichia coli recC* gene and of the *thyA-recC* intergenic region. *Nucleic Acids Res.* **14**, 4437–4451.
  20. Anderson, D. G. & Kowalczykowski, S. C. (1997). The translocating RecBCD enzyme stimulates recombination by directing RecA protein onto ssDNA in a  $\chi$ -regulated manner. *Cell*, **90**, 77–86.
  21. Kowalczykowski, S. C., Dixon, D. A., Eggleston, A. K., Lauder, S. D. & Rehrauer, W. M. (1994). Biochemistry of homologous recombination in *Escherichia coli*. *Microbiol. Rev.* **58**, 401–465.
  22. Smith, G. R. (1990). RecBCD enzyme. In *Nucleic Acids and Molecular Biology* (Eckstein, F. & Lilley, D. M. J., eds), pp. 78–98, Springer-Verlag, Berlin, Germany.
  23. Spies, M., Amitani, I., Baskin, R. J. & Kowalczykowski, S. C. (2007). RecBCD enzyme switches lead motor subunits in response to  $\chi$  recognition. *Cell*, **131**, 694–705.
  24. Yu, M., Souaya, J. & Julin, D. A. (1998). The 30-kDa C-terminal domain of the RecB protein is critical for the nuclease activity, but not the helicase activity, of the RecBCD enzyme from *Escherichia coli*. *Proc. Natl Acad. Sci. USA*, **95**, 981–986.
  25. Yu, M., Souaya, J. & Julin, D. A. (1998). Identification of the nuclease active site in the multifunctional RecBCD enzyme by creation of a chimeric enzyme. *J. Mol. Biol.* **283**, 797–808.
  26. Bianco, P. R., Brewer, L. R., Corzett, M., Balhorn, R., Yeh, Y., Kowalczykowski, S. C. & Baskin, R. J. (2001). Processive translocation and DNA unwinding by individual RecBCD enzyme molecules. *Nature*, **409**, 374–378.
  27. Handa, N., Bianco, P. R., Baskin, R. J. & Kowalczykowski, S. C. (2005). Direct visualization of RecBCD movement reveals cotranslocation of the RecD motor after  $\chi$  recognition. *Mol. Cell*, **17**, 745–750.
  28. Spies, M., Bianco, P. R., Dillingham, M. S., Handa, N., Baskin, R. J. & Kowalczykowski, S. C. (2003). A molecular throttle: the recombination hotspot  $\chi$  controls DNA translocation by the RecBCD helicase. *Cell*, **114**, 647–654.
  29. Arnold, D. A. & Kowalczykowski, S. C. (2000). Facilitated loading of RecA protein is essential to recombination by RecBCD enzyme. *J. Biol. Chem.* **275**, 12261–12265.
  30. Goralenya, A. E. & Koonin, E. V. (1993). Helicases: amino acid sequence comparisons and structure–function relationships. *Curr. Opin. Struct. Biol.* **3**, 419–429.
  31. Dillingham, M. S., Spies, M. & Kowalczykowski, S. C. (2003). RecBCD enzyme is a bipolar helicase. *Nature*, **423**, 893–897.
  32. Taylor, A. F. & Smith, G. R. (2003). RecBCD enzyme is a DNA helicase with fast and slow motors of opposite polarity. *Nature*, **423**, 889–893.
  33. Roman, L. J., Eggleston, A. K. & Kowalczykowski, S. C. (1992). Processivity of the DNA helicase activity of *Escherichia coli* recBCD enzyme. *J. Biol. Chem.* **267**, 4207–4214.
  34. Roman, L. J. & Kowalczykowski, S. C. (1989). Characterization of the helicase activity of the *Escherichia coli* RecBCD enzyme using a novel helicase assay. *Biochemistry*, **28**, 2863–2873.
  35. Masterson, C., Boehmer, P. E., McDonald, F., Chaudhuri, S., Hickson, I. D. & Emmerson, P. T. (1992). Reconstitution of the activities of the RecBCD holoenzyme of *Escherichia coli* from the purified subunits. *J. Biol. Chem.* **267**, 13564–13572.
  36. Taylor, A. F. & Smith, G. R. (1995). Monomeric RecBCD enzyme binds and unwinds DNA. *J. Biol. Chem.* **270**, 24451–24458.
  37. Wong, C. J., Lucius, A. L. & Lohman, T. M. (2005). Energetics of DNA end binding by *E. coli* RecBC and RecBCD helicases indicate loop formation in the 3'-single-stranded DNA tail. *J. Mol. Biol.* **352**, 765–782.
  38. Farah, J. A. & Smith, G. R. (1997). The RecBCD enzyme initiation complex for DNA unwinding: enzyme positioning and DNA opening. *J. Mol. Biol.* **272**, 699–715.
  39. Singleton, M. R., Dillingham, M. S., Gaudier, M., Kowalczykowski, S. C. & Wigley, D. B. (2004). Crystal structure of RecBCD enzyme reveals a machine for processing DNA breaks. *Nature*, **432**, 187–193.
  40. Lucius, A. L. & Lohman, T. M. (2004). Effects of temperature and ATP on the kinetic mechanism and kinetic step-size for *E. coli* RecBCD helicase-catalyzed DNA unwinding. *J. Mol. Biol.* **339**, 751–771.
  41. Lucius, A. L., Vindigni, A., Gregorian, R., Ali, J. A., Taylor, A. F., Smith, G. R. & Lohman, T. M. (2002). DNA unwinding step-size of *E. coli* RecBCD helicase determined from single turnover chemical quenched-flow kinetic studies. *J. Mol. Biol.* **324**, 409–428.
  42. Lucius, A. L., Wong, C. J. & Lohman, T. M. (2004). Fluorescence stopped-flow studies of single turnover kinetics of *E. coli* RecBCD helicase-catalyzed DNA unwinding. *J. Mol. Biol.* **339**, 731–750.
  43. Ali, J. A. & Lohman, T. M. (1997). Kinetic measurement of the step-size of DNA unwinding by *Escherichia coli* UvrD helicase. *Science*, **275**, 377–380.
  44. Lucius, A. L., Maluf, N. K., Fischer, C. J. & Lohman, T. M. (2003). General methods for analysis of sequential “*n*-step” kinetic mechanisms: application to single turnover kinetics of helicase-catalyzed DNA unwinding. *Biophys. J.* **85**, 2224–2239.
  45. Bianco, P. R. & Kowalczykowski, S. C. (2000). Translocation step size and mechanism of the RecBC DNA helicase. *Nature*, **405**, 368–372.
  46. Wong, C. J. & Lohman, T. M. (2008). Kinetic control of  $Mg^{2+}$ -dependent melting of duplex DNA ends by *E. coli* RecBC. *J. Mol. Biol.* **378**, 759–775.
  47. Wong, C. J., Rice, R. L., Baker, N. A., Ju, T. & Lohman, T. M. (2006). Probing 3'-ssDNA loop formation in

- E. coli* RecBCD/RecBC–DNA complexes using non-natural DNA: a model for “chi” recognition complexes. *J. Mol. Biol.* **362**, 26–43.
48. Dillingham, M. S., Webb, M. R. & Kowalczykowski, S. C. (2005). Bipolar DNA translocation contributes to highly processive DNA unwinding by RecBCD enzyme. *J. Biol. Chem.* **280**, 37069–37077.
49. Perkins, T. T., Li, H. W., Dalal, R. V., Gelles, J. & Block, S. M. (2004). Forward and reverse motion of single RecBCD molecules on DNA. *Biophys. J.* **86**, 1640–1648.
50. Mascotti, D. P. & Lohman, T. M. (1995). Thermodynamics of charged oligopeptide–heparin interactions. *Biochemistry*, **34**, 2908–2915.
51. Gray, D. M., Hung, S. H. & Johnson, K. H. (1995). Absorption and circular dichroism spectroscopy of nucleic acid duplexes and triplexes. *Methods Enzymol.* **246**, 19–34.
52. Amundsen, S. K., Taylor, A. F., Chaudhury, A. M. & Smith, G. R. (1986). *recD*: the gene for an essential third subunit of exonuclease V. *Proc. Natl Acad. Sci. USA*, **83**, 5558–5562.
53. Taylor, A. F. & Smith, G. R. (1985). Substrate specificity of the DNA unwinding activity of the recBC enzyme of *Escherichia coli*. *J. Mol. Biol.* **185**, 431–443.
54. Lohman, T. M., Chao, K., Green, J. M., Sage, S. & Runyon, G. (1989). Large-scale purification and characterization of the *Escherichia coli* *rep* gene product. *J. Biol. Chem.* **264**, 10139–10147.
55. Wong, I., Chao, K. L., Bujalowski, W. & Lohman, T. M. (1992). DNA-induced dimerization of the *Escherichia coli* *rep* helicase. Allosteric effects of single-stranded and duplex DNA. *J. Biol. Chem.* **267**, 7596–7610.
56. Williams, D. J. & Hall, K. B. (2000). Monte Carlo applications to thermal and chemical denaturation experiments of nucleic acids and proteins. *Methods Enzymol.* **321**, 330–352.